Study on Omega Signals Observed by Poynting Flux Analyzer on board the Akebono Satellite

doi: https://doi.org/10.14569/IJACSA.2016.071009

Study on Omega Signals Observed by Poynting Flux Analyzer on board the Akebono Satellite

Graduate School of

Natural Science & Technology

Kanazawa University

Division of

Electrical Engineering and

Computer Science

by

I Made Agus Dwi Suarjaya

March 21, 2017

Abstract

The Akebono satellite was launched in 1989 to observe the Earth's magnetosphere and plasmasphere. Omega was a navigation system with 8 ground stations transmitter and had transmission pattern that repeats every 10 s. From 1989 to 1997, the PFX on board the Akebono satellite received signals at 10.2 kHz from these stations. Huge amounts of PFX data became valuable for studying the propagation characteristics of VLF waves in the ionosphere and plasmasphere. In this study, we developed automatic detection of Omega signals from the PFX data. We were able to detect the omega signals and showed that they propagate to the opposite hemisphere along the Earth's magnetic field lines. From 1989 to 1997, we detected 127,900 and 476,134 signals in the PFX data of magnetic and electric field, respectively, and demonstrated that the proposed method is powerful enough for the statistical analyses. The signals transmitted from almost the same latitude in geomagnetic coordinates propagated differently depending on the geographic latitude. The Omega signal tended to propagate farther on the nightside and when solar activity was at a minimum, the Omega signal propagated at a higher intensity level and farther from the transmitter station.

1. Introduction

The Earth's plasmasphere is located at the inner part of the magnetosphere and is mainly filled with cold plasma. VLF waves such as whistlers (Carpenter, 1963) and Omega signal are strongly affected by the electron density profile. Major species of ions in the plasmasphere are protons, helium ions, and oxygen ions and composition ratio of these ions plays an important role in the propagation effect of VLF waves such as subprotonospheric whistler and magnestospherically reflected whistler (Kimura, 1966). Hence it is very important to clarify the spatial distribution of electron density as well as ion constituents in the magnetosphere to understand the propagation characteristics of VLF waves. In other words, propagation characteristics of the VLF wave could be an important clue to study the electron density profile in the magnetosphere. Because the global plasmaspheric electron density changes day by day, it is important to assess the trend of this change using statistical study of electromagnetic wave propagation over several years. In addition, observing signals from artificial transmitters are worth analyzing for such a purpose because these transmitters were constantly transmitting signals with constant power; thus, it is possible to analyze the extent of change in the wave propagation. This technique has been used to estimate the ionospheric topside and bottom-side profile with sounder (Reinisch et al., 2001; Ganguly et al., 2001) which is capable to check the ionospheric peak parameters such as density, height and peak shape (Pulinets et al., 2001).

Japan has launched a satellite nicknamed Akebono (EXOS-D) in 1989 to observe the Earth's magnetosphere and plasmasphere. The satellite consists of several scientific instruments such as particle detectors, magnetometer, electric field detector, plasma wave instruments and auroral camera. The VLF instrument is one of the instruments on board Akebono to measure VLF plasma waves and the Poynting flux Analyzer subsystem (PFX) is a subsystem of the VLF instrument (Kimura et al., 1990). The PFX is a waveform receiver that measures three components of magnetic fields and two components of electric fields. The waveforms generated from the PFX have band-width of 50 Hz at fixed center frequency from 100 Hz to 12.75 kHz. The Wide Dynamic Range Amplifier (WIDA) hybrid ICs are equipped for the gain control to achieve wide measurable dynamic range (Kimura et al., 1990).

Omega system was a navigation system to provide a navigational aid for domestic aviation and oceanic shipping with 8 ground station transmitter located at Norway, Liberia, Hawaii, North Dakota, La Reunion Island, Argentina, Australia, and Japan (Morris et al., 1994). The PFX had been observed Omega signals transmitted from these 8 ground stations around 1989-1997. The PFX captured one of the common frequency of Omega signal, that is the 10.2 kHz. Later on, this navigation system was shut down in 1997 in favor of the GPS system. Omega signal data captured by the PFX on board the Akebono have been used to estimate the global plasmaspheric electron density deduced from in situ electron density and wave normal directions (Sawada et al., 1993). In particular, a tomographic electron density profile could be determined by calculating the Omega signal propagation path using a ray-tracing method. This method could estimate the propagation path using 1-h data of single satellite observation (Kimura et al., 2001). The algorithm was further improved with a flexible method and novel stochastic algorithm. This enabled separate estimation of the effects of the ionosphere and plasmasphere (Goto et al., 2003).

Because the transmission pattern of frequency, the time, and the location of each station is known, we can easily distinguish the signal source. We can then determine many

propagation properties such as attenuation ratio, propagation direction, propagation time (delay time) from the transmission station, and the observation point along the satellite trajectories. Such parameters depend strongly on the plasma parameters along the propagation path. Therefore, it is valuable to analyze such propagation characteristics of VLF waves in the ionosphere and plasmasphere statistically using the long-term observation data. We investigate statistical features of the Omega signals detected by the PFX from 1989 to 1997. To achieve this purpose, we picked up Omega signals from the enormous amount of the PFX data using an automatic detection program developed by Suarjaya et al. (2016). The methods used are consist of FFT analyses, determination of the stations that transmitted the signals, estimation of delay time, discrimination of signal existence, and estimation of signal intensity. We also added some error detection and efficient processing methods for rapid analysis. The results for intensity, delay time, and local time-dependence analysis are presented as geographic and geomagnetic maps.

1.1 PFX Instrument

The PFX subsystem of the Akebono satellite measured three components of magnetic fields (B_1, B_2, and B_3) and two components of electric fields (E_x and E_y). The subsystem comprised five-channel triple-super-heterodyne receivers with an output bandwidth of 50 Hz. It also contained a local oscillator that could be stepped or fixed at a specific center frequency with a range of 100–12.75 kHz and was equipped with a Wide Dynamic Range Amplifier (WIDA) hybrid IC to control the gain in the dynamic range for more than 80 dB (Kimura et al., 1990). The WIDA hybrid IC automatically checked the averaged signal level every 0.5 s and the gain of each channel could be changed independently in 25 dB steps from 0 dB up to 75 dB. For our study, we use B_X, B_Y, B_Z, E_X and E_Y in static coordinate system converted from B_1, B_2, B_3, E_x and E_y obtained in the antenna coordinate system fixed to the spinning satellite as defined in Kimura et al. (1990). The static coordinate system is referred to the direction of the geomagnetic field (the geomagnetic field line is in the X-Z plane and Y is perpendicular to the X-Z plane) and the direction of the sun (Z-axis).

1.2 Omega System

The Omega signal is very low frequency (VLF) signal between 10 and 14 kHz transmitted by the Omega navigation system that was operational in 1971. Before it shut down in 1997, its purpose was to provide a navigational aid for domestic aviation and oceanic shipping. Omega receiver determines location based on the phase of the signal from two or more of the Omega stations (Morris et al., 1994). This Omega signal was transmitted from eight ground stations with each station transmitting a unique pattern, based on which our analyzer software could determine the source of the signal. The location of these Omega stations are Norway (NW), Liberia (LB), Hawaii (HW), North Dakota (ND), La Reunion Island (LR), Argentina (AZ), Australia (AS), and Japan (JP).

2. Automatic Detection of Omega Signal

2.1 FFT Analysis

The PFX data is stored as waveforms sampled at rate of 320 Hz. For FFT analysis, we used FFT size of 32. Therefore, the time resolution was 100 ms and the frequency resolution was 10 Hz. To improve the accuracy of delay time detection, we applied an overlap-add FFT

every three sample points for a higher time resolution (~9.4 ms) when the first signal was detected. Although PFX measured only two components of the electric field, we could derive another component (E_Z) if we assumed the measured signal as a single plane wave (Yamamoto et al., 1991). After we calculated the E_Z component, we could use it to calculate the absolute intensity of the electric field $|E|$ and the absolute intensity of the magnetic field $|B|$. We use dB (V/m) for the electric field measurement unit and dB (T) for the magnetic field measurement unit.

2.2 Signal Detection and Threshold Level Determination

We first estimated the raise time of each signal by comparing the average intensity of specific time frame to the threshold level, expecting a sudden increase in intensity. Second, we determined the transmission station by comparing the raise time with the transmission patterns of the eight Omega stations. At 0000 UT on January 1, 1972, the Omega and UTC scales were identical. However, we subsequently had to conduct a leap seconds calculation to synchronize the omega time and UTC because the Omega had no leap seconds like the UTC (Morris et al., 1994). On December 31, 1989, the Omega time led the UTC by 14 s. In the present study, we decided to detect the Omega signals at least 5 dB larger than the average intensity of ambient noise level of every 10 seconds duration (1 window) and at least 8 dB larger than the average intensity of ambient noise level surrounding the omega signal (upper and lower frequencies).

2.3 Delay Time Detection

We calculated the delay time of the signal by subtracting the transmission time of the station as shown in equation (1), where T_P denotes the intensity threshold (8 dB), t_d denotes delay time in seconds, P_n denotes average intensity strength of center frequency consist of 5 bins in frequency (10 Hz per bin) and 20 bins (~9.4 ms per bin) in time, P_u_n denotes average intensity strength of upper frequency consist of 5 bins in frequency and 20 bins in time, P_l_n denotes average intensity strength of lower frequency consist of 5 bins in frequency and 20 bins in time, t_0 denotes start time of the station's transmission, t_n denotes start time of P_n, and n denotes the iteration number for every 1 bin in time. Average intensity strength is calculated by averaging all of the bins for the parameter.

$$t_d = \begin{cases} t_n - t_0 & \text{if } \left(P\_u_n + P\_l_n\right)/2 + T_P < P_n \text{ and } \left(P_n - P_{n-1}\right) > T_P \\ 0 & \text{otherwise} \end{cases} \quad (1)$$

2.4 Signal Discrimination and Intensity Determination

In the next step, we determined signal existence by comparing the average intensity of the expected duration of the Omega signal with the surrounding intensity (higher and lower frequency points of the center frequency) after delay time detection. We determined signal existence and derived the signal intensity ($P_{\omega s}$) by using equation (2), where P_a denotes the average intensity strength of the upper frequency bins in decibels, P_b denotes the average intensity strength of lower frequency bins in decibels, P_s denotes the average intensity strength of center frequency bins in decibels, and P_w denotes average intensity strength of all bins in frequency and time for every 10 s duration (1 window) in decibels. P_a, P_b, and P_s consist of 5 bins in frequency, and variation in number of bins in time depends on the duration of the Omega signal for each station.

$$P_{\omega s} = \begin{cases} P_s & \text{if } \left(P_a + P_b\right)/2 + T_P < P_s \text{ and } \left(P_w + T_w\right) < P_s \\ 0 & \text{otherwise} \end{cases} \quad (2)$$

3. PFX Analyzer

We developed software to analyze the Omega signal data measured by the Akebono from 1989 to 1997. The software was written in Java programming language. It enables us to detect Omega signals automatically for several months or years and then show the results of electric and magnetic intensity and delay time for specific locations of longitude, latitude, and altitude on geomagnetic and geographic maps of the Earth. Analyses of local time dependence are also available. This analyzer connects to the Akebono orbit database and can be used to manually analyze each signal in real time by manipulating the navigation panel. To automatically analyze the CDF files for one month of data, we need 6–9 hours of processing time using an Intel Quad Core with a 3.324 GHz CPU and 4 GB of memory. The computational time depends on the number of available signal data and data size. Depending on the computer specifications, it is possible to run multiple instances of the analyzer to speed up the process.

4. Omega Signal Propagation Analysis

4. 1 Event Study

To demonstrate the reliability of our datasets and the automatic detection, in this section we present result of study from few interesting events. Figure 1 (a) and 1 (b) shows 1.5 hours of trajectory of the Akebono from the northern to southern hemisphere from 08:29:39.802 UT to 09:55:33.842 UT on October 18, 1989. During this period, Omega signals from the Norway station were continuously observed and 344 signals were detected in the electric field and 63 signals were detected in the magnetic field. The location of the Norway station is also shown as a small square in Figure 1 (a) and (b). The PFX data are not available between latitude 49°N to 26°N and 2°N to 6°S. This unavailable of data are shown as dashed lines in Figure 4.2 (a). Figure 1 (c) shows absolute intensities of magnetic fields, Figure 1 (d) shows electric fields, and Figure 1 (e) shows delay time of the Omega signals. The red curves indicate moving median over 20 points (detected events). The intensity of the magnetic field and electric field of the Omega signal is showing higher intensity in the northern hemisphere where the Norway station was located. The Norway station was located at latitude 56.42°N, and we can see higher signal intensity approximately −283 dB (T) for the magnetic field and approximately −125 dB (V/m) for the electrical field. The intensity then becomes lower for the electric field or disappears for the magnetic field near the equator at latitude 0°. The signal for the electric field then increased at approximately −145 dB (V/m) near the southern hemisphere because the signal could propagate along the Earth's magnetic field. The delay time is around 0.2 s in the northern hemisphere where the Norway station was located and then increased to more than 0.5 s as the trajectory of the Akebono satellite got closer to the southern hemisphere. This occurred because propagation along the Earth's magnetic field required more time compared with a direct propagation path. Figure 1 (f) shows the approximate distance based on a simple magnetic dipole model for the propagation path of the signal along the Earth's magnetic field (Luhmann and Friesen, 1979; Prölss, 2004). The calculated distances was from the Norway station to the observation point.

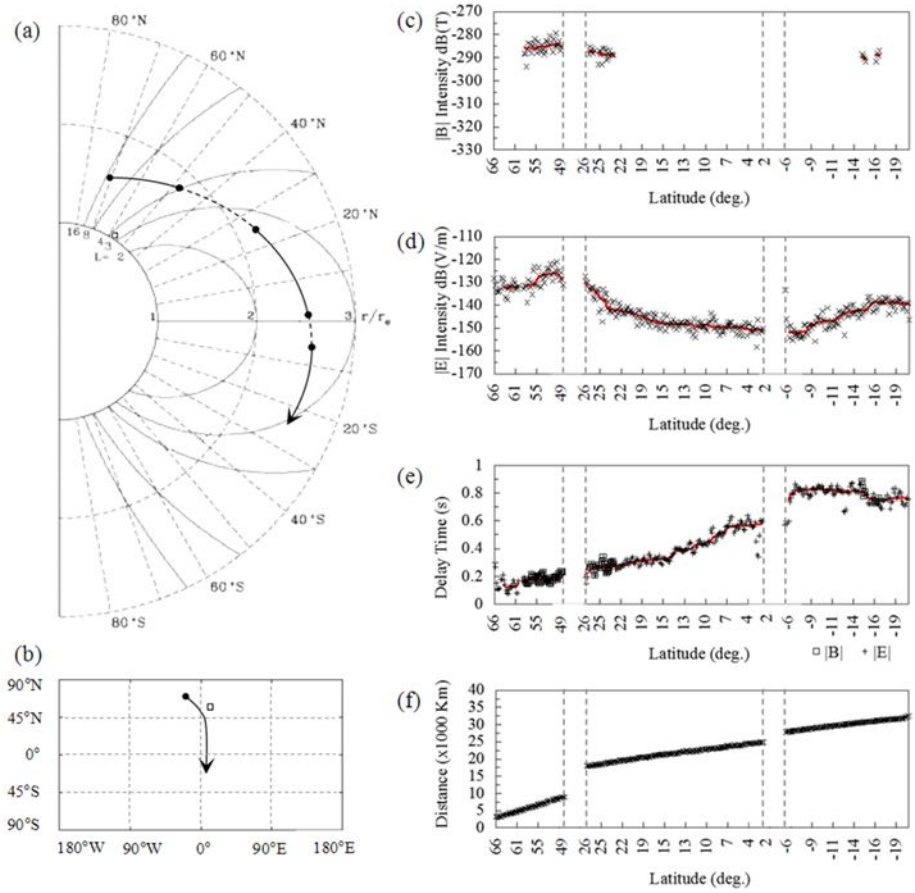

Figure 1. Observed Omega signal of Norway station 08:29:39.802 UT-09:55:33.842 UT on October 18, 1989.

4. 2 General characteristics of Omega signal propagation from Norway and North Dakota Stations

First we study the signal intensity just above the transmission station to evaluate how wide and how much the Omega signals penetrated through the ionosphere over the station. For this purpose, we restricted the PFX data obtained below 640 km in altitude. Figure 2 (a) shows the number of events used for the analysis just above the Norway station from October 1989 to September 1997, which was located at longitude 100.72°E and latitude 55.96°N in geomagnetic coordinates. Figure 2 (b) and Figure 2 (c) show the averaged intensity of the signals in electric and magnetic fields, respectively. White areas on the map indicate unavailability of PFX data. The location of the station is shown on the map indicated by rectangle in each panel. We divided the horizontal axis into 20 bins of longitude (5° for each bin) and the vertical axis into 20 bins of latitude (5° for each bin). The gray color in Figure 2 (b) and Figure 2 (c) indicates no event was detected either because of the intensity too low if compared to the threshold level or because of high noise which made the condition of detection became false. The number of event in Figure 2 (a) and signal intensities in Fig 2 (b) and Figure 2 (c) are indicated by color scales given at the right of each panel. It is also notable that the high-intensity area was located at ~10° northern part of the transmitter station. The center of the penetration region is located approximately at longitude 97°E and latitude 65°N in geomagnetic coordinates. The intensities at this point were approximately −265 dB(T) in magnetic field and −120 dB(V/m) in electric field, respectively. It was also found that the region where Omega signal penetrated the ionosphere covered a radius of ~3,900 km from the

center of the transmitter station, between approximately latitude 10°N to 80°N and longitude 70°E to 140°E in geomagnetic coordinates.

Figure 3 (a) shows the number of events used for the analysis just above the North Dakota station from October 1989 to September 1997, which was located at longitude 34.83°W and latitude 55.98°N in geomagnetic coordinates. White areas on the map indicate unavailability of PFX data, especially around the eastern part of the transmitter station. Figure 3 (b) and Figure 3 (c) show the averaged intensity of the signals in electric and magnetic fields, respectively. The gray color indicates no event was detected in that region. The Omega signal that penetrated the ionosphere and propagated along the Earth's magnetic field lines covered a radius of ~3000 km in the region around the transmitter station between approximately latitude 10°N to 70°N and longitude 5°E to 65°W in geomagnetic coordinates. A high-intensity area is visible immediately above the station transmitter at approximately −255 dB(T) in the magnetic field and approximately −110 dB(V/m) in the electric field. Compared to the Norway station, different regions of high-intensity signal are apparent, where the center of the penetration region is located approximately at longitude 34°W and latitude 55°N in geomagnetic coordinates, despite both stations being at the same latitude in geomagnetic coordinates, approximately 55.9°N.

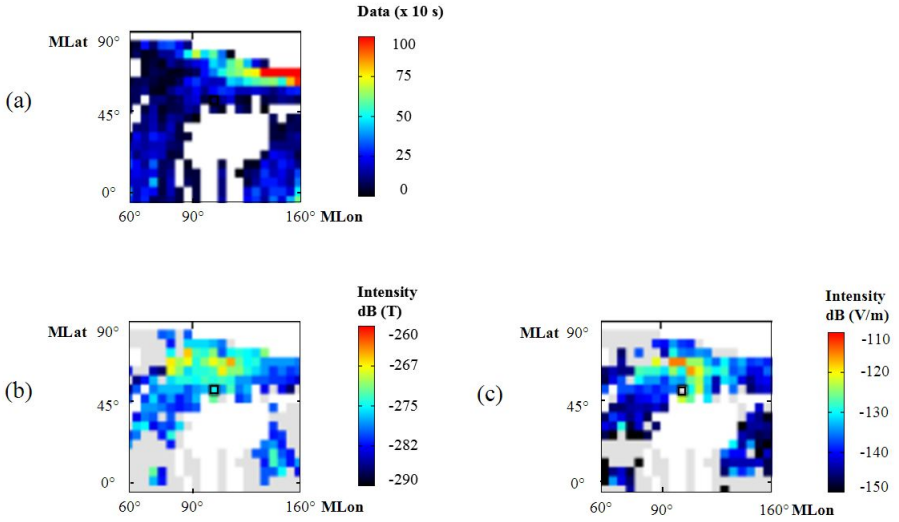

Figure 2. Propagation for Norway Station<640 Km in M-Field (a) and in E-Field (b)

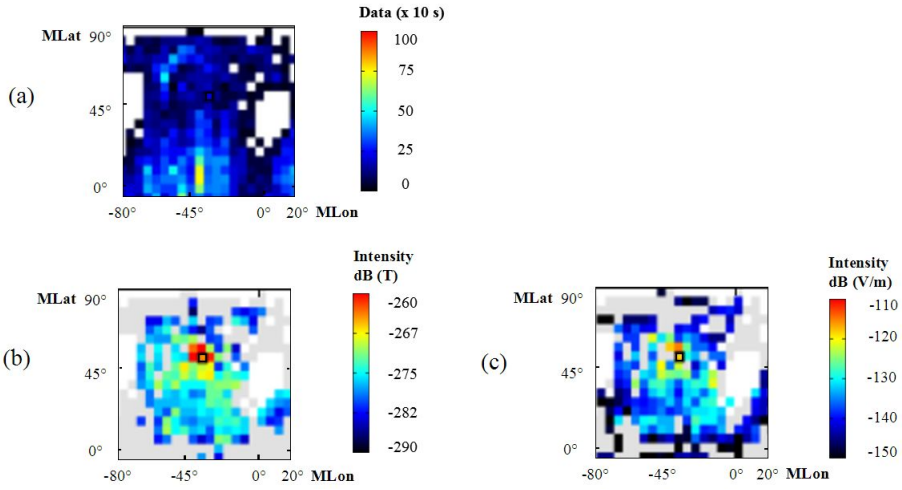

Figure 3. Propagation for North Dakota Station<640 Km in M-Field (a) and in E-Field (b)

4. 3 Magnetic Local Time Dependence

In this section, we examined the transmittance of Omega signals as a function of magnetic local time to evaluate the attenuation effect of the ionosphere and plasmasphere. Using the Magnetic Local Time (MLT) of the observation points, we separated the intensity maps every 3 hours. We compared the results using the data obtained around the Norway station and the North Dakota station. Figure 4 shows the Omega signal intensity transmitted by the Norway station from October 1989 to September 1997 in geomagnetic coordinate without any altitude data restriction.The vertical axis indicates geomagnetic latitude and horizontal axis indicates geomagnetic longitude, and 8 panels correspond to the sections separated every 3 MLTs. For the longitude, it is centered at the location of the station with range of 100° (±50° centered at the station). The rectangle on the map indicates the location of the station which was located at longitude 100.72°E and latitude 55.96°N. The transition of the intensity level demonstrates that the nightside has a high intensity level at approximately −115 dB(V/m) in the electric field and approximately −265 dB(T) in the magnetic field. The dayside has the lowest intensity level, of approximately −120 dB(V/m) in the electric field and approximately −270 dB(T) in the magnetic field. In addition, the dayside (MLT 9-15) clearly exhibits narrow propagation with only ~50° width of range in longitude compared to the other MLT sides.

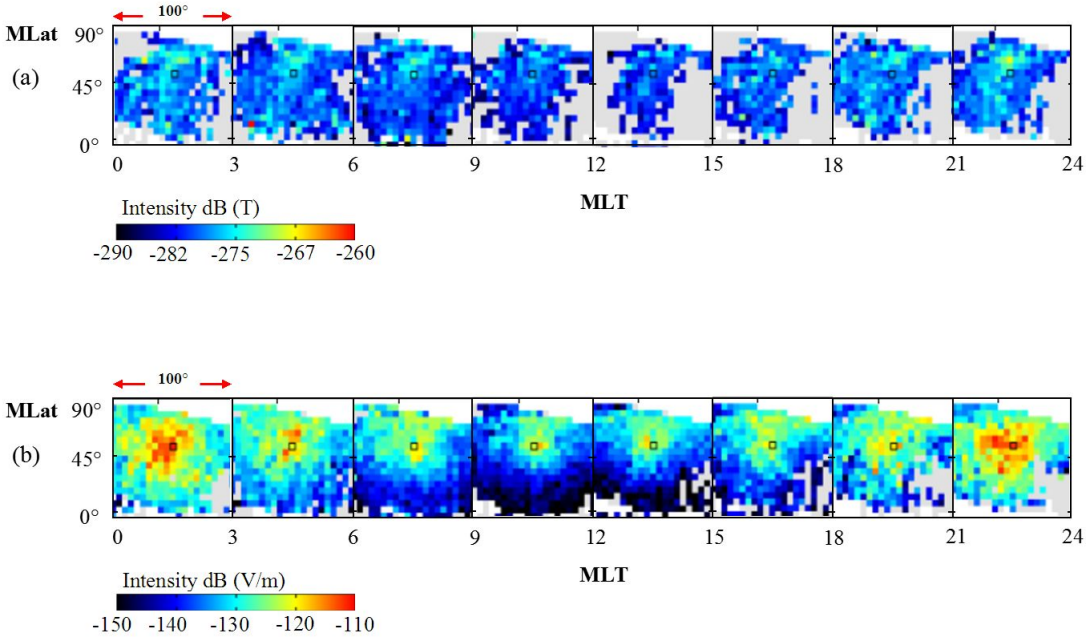

Figure 4. Propagation from Norway Station based on Local Time in M- Field (a) and E-Field (b)

4. 4 Seasonal Variation

In this section, we study the seasonal variation of Omega signals propagation to evaluate the trend of propagation characteristic for each season. In the analyses, we separated the eight years of data into four seasons centered at the equinox and solstice of each year. Data range for the March equinox is February 1 to April 30, June solstice is May 1 to July 31, September equinox is August 1 to October 31 and December solstice is November 1 to January 31.

Figure 5 Figure 4.12 shows the spatial distribution of Omega signals transmitted by the Norway station from October 1989 to September 1997. The upper four panels show magnetic

intensity and the lower four panels show electric intensity. We plot the intensity map taking its vertical axis as indicate invariant latitude (ILAT) of the observation point and the horizontal axis as geomagnetic longitude. The rectangle on the map indicates the location of the station. It was found that the high-intensity region was deviated 10° to higher invariant latitude from the transmitter. Intensities in the high-intensity region were approximately -275 dB(T) for the magnetic field and approximately -117 dB(V/m) for the electric field. Intense signals were detected in the wider region in December solstice, while the high-intensity region became the smallest in June solstice. In addition, it is very interesting that, the high-intensity region in electric field was located only at 10° higher invariant latitude from the transmitter in June solstice. But it gradually spread northward (higher latitude) in September equinox and became the widest in December solstice. The region shrunk southward again in March equinox..

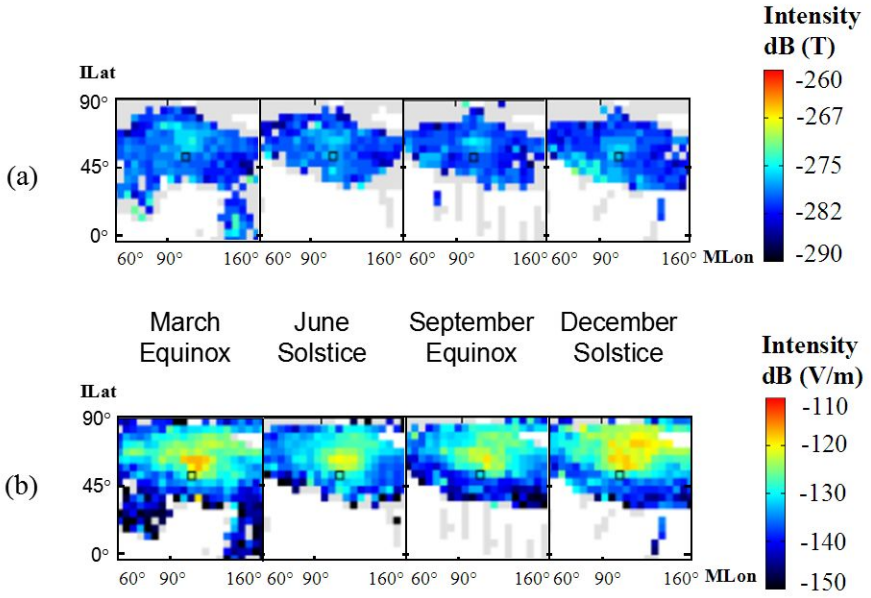

Figure 5. Seasonal Propagation from Norway Station in M-Field (a) and E-Field (b)

4.5 Annual Variation

Finally we study annual variation of propagation characteristics to evaluate the effects of solar activity. We separated the data and illustrated the results for each year. Figure 6 shows the Omega signal propagation pattern transmitted by the Norway station from October 1989 to September 1997 in geomagnetic coordinate. The vertical axis indicates latitude and horizontal axis indicates longitude with range of 100° (±50° centered at the station), and 9 panels corresponding to 1989 to 1997 are shown. The rectangle on the map indicates the location of the station. We used data below an altitude of 8200 km for the entire year because the satellite's altitude decreased every year and no data are available in 1997 above that altitude. Between 1989 and 1992, the intensity level was low; from 1993 to 1997, the average intensity level was higher and the propagation region of the Omega signal was wider. Based on sunspot cycle data (NASA/Marshall Solar Physics, 2016), the sunspots number on the surface of the sun increased between 1989 and 1992 during the solar maximum period, while it decreased between 1993 and 1997 corresponding to the solar minimum period. We noticed that this phenomenon significantly affected the propagation and penetration of Omega signal in the ionosphere. The Omega signal propagation intensity near the station during the solar maximum (1991) was approximately −280 dB(T) in the magnetic field and approximately −120 dB(V/m) in the electric field. During the solar minimum (1996), higher intensity level

that propagated wider and farther from the transmitter station is apparent, approximately −270 dB(T) in the magnetic field and approximately −115 dB(V/m) in the electric field. Based on these maps, the coverage radius and intensity strength of the Omega signal that penetrated and propagated in the ionosphere altered by a few thousand kilometers every year.

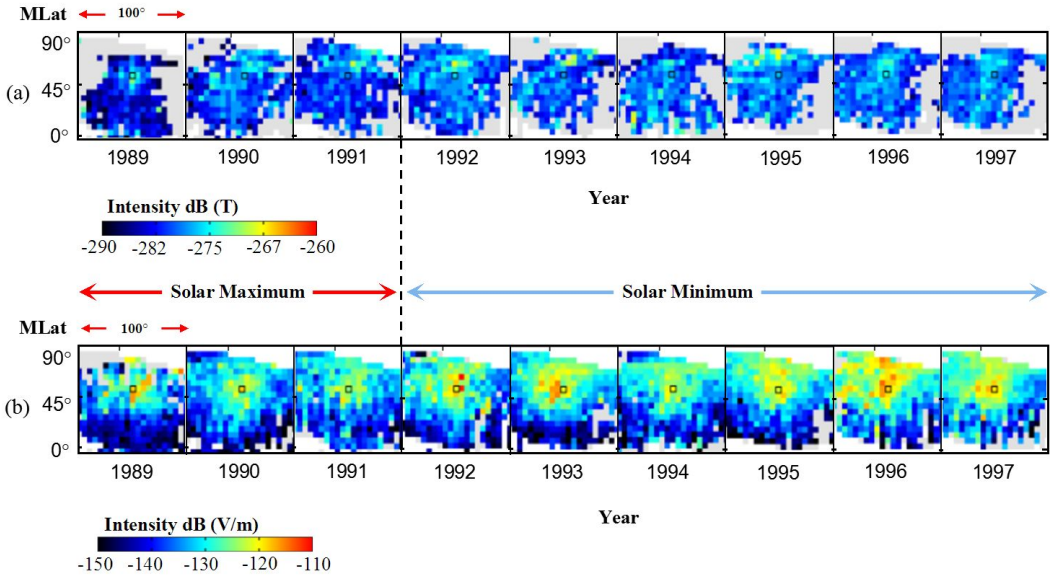

Figure 6. Annual Propagation from Norway Station in M-Field (a) and E-Field (b)

5. Conclusions

In this study, we developed an advanced detection algorithm for continuous processing of large amounts of data measured for several years by the PFX subsystem on board the Akebono satellite. The algorithm enables us to distinguish noise and real Omega signals and detect errors in order to produce more accurate results. Compared to manual analysis, automatic detection can be accomplished with short periods of processing time and does not require human intervention in the process.

We studied the high–middle-latitude Omega stations located at Norway and North Dakota and evaluated how wide and how much the Omega signals penetrated through the ionosphere over the station. Our analysis revealed that, for stations located at almost the same latitude in geomagnetic coordinates, the Omega signal propagated along the Earth's magnetic field differently.

Second we examined the transmittance of Omega signals as a function of magnetic local time to evaluate the attenuation effect of the ionosphere and plasmasphere. We found that the Omega signal tended to propagate farther in the nightside, where the electron density in the ionosphere was lower than in the dayside.

We also studied on the seasonal variation of Omega signals to evaluate the trend of propagation characteristic. We found that intense signals from Norway station were detected in the wider region in December solstice, while the high-intensity region became the smallest in June solstice.

Finally, we studied the annual variation of the propagation characteristics of Omega signals to evaluate the effects of solar activity. We found that in 1991, when solar activity was at a maximum, the Omega signal propagated at a lower intensity level; in contrast, in 1996 when solar activity was at a minimum, the Omega signal propagated at a higher intensity level and farther from the transmitter station. We assumed that plasmaspheric electron density and temperatures affected the propagation of the Omega signal.

As was described in the introduction, quantitative study of the Omega signals using the eight years of PFX data from October 1989 to September 1997 is quite important to evaluate the attenuation ratio of VLF waves propagating in the ionosphere and plasmasphere as a function of magnetic local time, season, annual solar activity. In the future, extensive study of the delay time and wave normal direction are necessary to clarify the global features of the ionosphere and plasmasphere quantitatively.

References

Carpenter, D.L., 1963. Whistler evidence of a 'knee' in the magnetospheric ionization density profile, J. Geophys. Res., 68, 1675–1682.

Ganguly, S., V. Wickwar , and J.M. Goodman, 2001. New generation topside sounder , Radio Science, 36, 5, 167-1179.

Goto, Y., Y. Kasahara, T. Sato, 2003. Determination of plasmaspheric electron density profile by a stochastic approach, Radio Science, 38(3), 1060, doi:10.1029/2002RS002603.

Kimura, I., 1966. Effects of Ions on Whistler-Mode Ray Tracing, Radio Science, 1, pp.269-283.

Kimura, I., K. Hashimoto, I. Nagano, T. Okada, M. Yamamoto, T. Yoshino, H. Matsumoto, M. Ejiri, K. Hayashi, 1990. VLF Observation by the Akebono (EXOS-D) Satellite, Journal of Geomagnetism and Geoelectricity, 42, pp. 459-478.

Kimura, I., Y. Kasahara, H. Oya, 2001. Determination of global plasmaspheric electron density profile by tomographic approach using Omega signals and ray tracing, Journal of Atmospheric and Solar-Terrestrial Physics, 63, 1157–1170.

Luhmann, J. G., and L. M. Friesen, A simple model magnetosphere, 84, 4405-4408, 1979.

Morris, P. B., R. R. Gupta, R. S. Warren, P. M. Creamer, 1994. Omega Navigation System Course Book, Vol. 1, National Technical Information Service, Springfield, Virginia, 434pp.

NASA/Marshall Solar Physics, 2016. http://solarscience.msfc.nasa.gov/SunspotCycle.shtml

Prölss, G. W., 2004. Physics of the Earth's space environment: an introduction, Springer.

Pulinets, S.A., et al., 2001. MIR Space Station Topside Sounding near Taiwan, TAO, Vol. 12, No. 3, 525-536.

Reinisch, B.W., X. Huang, 2001. Deducing topside profiles and total electron content f rom bottomside ionograms, Advances in Space Research, 27, 1, 23-30.

Sawada, A., T. Nobata, Y. Kishi, I. Kimura, 1993. Electron Density Profile in the Magnetosphere Deduced From in Situ Electron Density and Wave Normal Directions of Omega Signals Observed by the Akebono (EXOS D) Satellite, Journal of Geophysical Research, 98, A7, 11267-11274.

Suarjaya, I.M.A.D., Y. Kasahara, Y. Goto, 2016. Automatic Detection of Omega Signals Captured by the Poynting Flux Analyzer (PFX) on Board the Akebono Satellite, International Journal of Advanced Computer Science and Applications, 7(10), 67-74, doi:10.14569/IJACSA.2016.071009.

平成 29 年　2 月　1 日

学位論文審査報告書（甲）

1．学位論文題目（外国語の場合は和訳を付けること。）

Study on Omega Signals Observed by Poynting Flux Analyzer on board the Akebono Satellite

（和訳）あけぼの衛星ポインティングフラックス測定器で観測されたオメガ信号の研究

2．論文提出者　(1) 所　　属　電子情報科学　　専攻

(2) 氏（ふり）名（がな）　I Made Agus Dwi Suarjaya（イ マデ アグス デウィ スアルジャヤ）

3．審査結果の要旨（600～650 字）

平成 29 年 2 月 1 日午前に第 1 回学位論文審査委員会を開催した後、同日午後に口頭発表を実施した。その直後に、第 2 回審査委員会を開いて慎重審議を行った結果、以下の通り判定した。なお、口頭発表における質疑を最終試験に代えるものとした。

地球近傍のプラズマ環境は、太陽活動・季節・ローカルタイムなどに依存し変動する。本研究は、電離層を透過しプラズマ圏を伝搬する VLF 帯の船舶航行用ナビゲーション信号「オメガ」を、科学衛星あけぼの搭載ポインティングフラックス測定器で計測したデータを解析し、その伝搬特性を明らかにした。まず、あけぼの衛星が計測したオメガ信号を検出し、世界に 8 局設置されていたどの送信局からの信号かを自動同定し、その電磁界強度や伝搬遅延時間を求める解析システムを開発した。次に同システムを用いて、約 9 年間の計測データを統計解析し、プラズマ圏内における信号の伝搬経路や減衰特性の太陽活動・季節・ローカルタイム依存性を定量的に明らかにした。宇宙プラズマ中を伝搬する VLF 帯電波の屈折・減衰特性は、伝搬媒質であるプラズマ密度のグローバルな空間・時間変動を知る有力なパラメータであるが、あけぼの衛星が長期間に渡り計測したデータを網羅的解析し、VLF 帯電波の伝搬特性を定量的に示した同研究は、世界的にも大変重要な成果と言える。以上より、本論文は博士（工学）に値すると判定した。

4．審査結果　(1) 判　　定（いずれかに○印）　（合　格）・　不合格

(2) 授与学位　　博　士（　工学　）